Open Access

Journal of Energy and Power Technology

LIDSEN Publishing Inc.

Original Research

Experimental Study and Kinetic Modeling of Agro-Industrial Wastes for Conversion to Fuel Gas via the Boudouard Reaction

Despina Vamvuka *, Stelios Sfakiotakis, Elpida Patlaka

School of Mineral Resources Engineering, Technical University of Crete, Chania, 73100, Greece; E-Mails: dvamvouka@tuc.gr; ssfakiotakis@tuc.gr; elpidapatlaka@gmail.com

* **Correspondence:** Despina Vamvuka; E-Mail: dvamvouka@tuc.gr

Academic Editor: Alissara Reungsang

Journal of Energy and Power Technology
2025, volume 7, issue 1
doi:10.21926/jept.2501004

Received: February 15, 2024
Accepted: January 16, 2025
Published: January 24, 2025

Abstract

Independent parallel reactions (IPR) and distributed activation energy (DAEM) kinetic models were developed and compared for the combined pyrolysis-gasification of two agro-industrial waste materials. The aim was to recycle greenhouse gas carbon dioxide for mitigating emissions, to evaluate the thermal behavior, reactivity, conversion and product composition in terms of structural/chemical characteristics of the fuels, and to provide accurate kinetic parameters useful in the scaling-up of the process. The experiments were conducted in a thermogravimetric system, coupled with a mass spectrometer. Both models accurately represented the pyrolysis process by three first-order reactions with deviation values ranging from 1.6% to 2.4%. For the gasification process, one pseudo-component described the process successfully, with deviation values of 2.3-5%. The IPR model provided a superior fit. Activation energy values estimated by the DAEM model were higher than those predicted by the IPR model.

Keywords

Carbon dioxide; pyrolysis; gasification; kinetics

1. Introduction

One of the major greenhouse gases responsible for global warming and negative climate change is carbon dioxide. Annual emissions from industry have reached 36.3 Gt [1]. Consequently, decarbonized energy policies worldwide require the implementation of negative-CO_2 emission technologies. The combustion of fossil fuels for power generation releases significant quantities of carbon dioxide and other hazardous species, leading to serious environmental issues. Conversely, utilizing biomass resources, which are regarded as CO_2-neutral and are widely available at low cost in most countries, is an attractive route not only for reducing the carbon footprint but also for recycling waste materials within the framework of a circular economy [2].

As an alternative to combustion, gasification is a flexible, highly efficient, and environmentally friendly process, producing syngas suitable for power generation, biofuels, and chemicals [3-6]. If the gasifying agent is carbon dioxide from residual gas streams then the process provides a potential solution to the greenhouse gas effect and the sequestration of carbon dioxide, offering at the same time marketable gaseous fuels. In a typical fixed bed gasifier, the feedstock is dried and pyrolyzed by flue gases, whereas the heat for its gasification is supplied by its partial oxidation with air. Thus, the reactivity of the fuel towards carbon monoxide gas, via the Boudouard reaction ($C + CO_2 \rightarrow 2CO$), depends to a great extent, apart from the composition of organic matter and ash, temperature and pressure, on the pyrolysis conditions affecting the structural properties and the aromaticity of char. An increased pore volume, a less ordered aromatic structure, and alkali/alkaline earth species have been found to enhance reactivity [3, 6-9]. In the case of fuels with high amounts of inherent alkali, operating the systems below 1000°C is recommended to avoid slagging/fouling problems [10, 11].

In order to optimize the gasification process and to design and operate industrial conversion systems efficiently, mathematical modeling describing the reaction rate during the thermochemical transformation of biomass materials should be implemented. The complexity of transforming a wide variety of solid biomass fuels to liquid and gaseous products under diverse operating conditions has led to developing various kinetic models, considering different reaction schemes such as single reactions, series of competing/consecutive reactions, parallel independent reactions, or combinations of them. The most known models are the iso-conversional models, the volume reactor model (VRM), the shrinking core model (SCM), the random pore model (RPM), the independent parallel reactions model (IPR) and the distributed activation energy (DAEM) model [3, 4, 9, 12-17]. Iso-conversional models are limited to qualitative results; the SCM is limited to the particle size of the feedstock, the RPM model is very complex, whereas a mathematical compensation effect has been reported for the IPR and DAEM models, especially at high heating rates [18].

The above models have been initially developed for coal gasification and applied to biomass materials only in recent years. Most previous investigations focused on iso-conversional models for the pyrolysis of agricultural biomass under pure nitrogen or the gasification under pure carbon dioxide [13-15, 18], and quite a few focused on SCM, VRM and RPM models for the carbon dioxide gasification of woody fuels [4, 9, 16, 19]. As already mentioned, SCM, VRM, and RPM models are intricate and possess limitations. On the other hand, iso-conversional models are based on numerical approximations, assume first-order reactions to take place, and often produce unreliable results. The IPR and DAEM models have been applied far less, excluding the authors, for coal or lignocellulosic chars [4, 9].

An extended IPR model linked the number of constituents of lignocellulosic materials and their properties during pyrolysis to the characterization of the materials [20]. A revised workflow for determining the amounts of biomass constituents, combining thermogravimetric analysis (TGA) under a nitrogen atmosphere with analyses of extractives and ash, using the IPR model, showed improved composition accuracy using a rapid TGA-based approach [21]. Activation energy values derived by IPR modeling of coconut fiber or shell pyrolysis varied between 79 kJ/mol-196 kJ/mol [22] and 79 kJ/mol-145 kJ/mol [23], respectively. Concerning the DAEM model, the pyrolysis of agricultural materials was found to pass through many multifaceted reaction mechanisms, with apparent activation energies 170.5-196.1 kJ/mol [24]. Corresponding values for coconut husk ranged from 141 kJ/mol to 230 kJ/mol [25]. Activation energies of a double DAEM model, describing the pyrolysis of palm kernel shell by two sub-processes, varied between 140 kJ/mol and 210 kJ/mol [26]. A DAEM model with Weibull distribution applied to the pyrolysis of rice straw and cotton stalk provided improved flexibility [27]. The application of IPR and DAEM models to the gasification process is scarce. Recently, kinetic modeling of the steam gasification of yak manure was only addressed using the DAEM model. For the pyrolysis stage, the activation energy associated was about 175 kJ/mol whereas for the char condensation stage and steam-char reaction, these values were 215 kJ/mol and 307 kJ/mol, respectively [28].

To the best of our knowledge, there is a lack of data on comparison between the IPR and DAEM models for combined pyrolysis-gasification under an atmosphere of residual carbon dioxide only, considering n-th order mechanisms. Furthermore, the combined process has not been reported so far for agro-industrial wastes, which are of high interest in many countries. In order to evaluate their potential for energy or product conversion, a comprehensive analysis of the properties and thermal behavior is necessary, due to their diverse characteristics in conjunction with a detailed assessment of process kinetics. According to the above discussion, the objectives of the current study were to develop and compare the IPR and DAEM kinetic models for the combined pyrolysis-gasification of two agro-industrial waste materials, sunflower pomace, and cotton residues. The aim was to recycle greenhouse gas carbon dioxide for mitigating emissions, to evaluate the thermal behavior, reactivity, conversion and product composition in terms of structural/chemical characteristics of the fuels, and to provide accurate kinetic parameters functional in the scaling-up of the process. The experiments were conducted in a thermogravimetric/differential thermogravimetric (TG/DTG) system, coupled with a mass spectrometer (MS).

2. Experimental

2.1 Raw Fuels and Characterization

The agro-industrial wastes selected for this study were sunflower pomace obtained after oil extraction (SP) and cotton residues resulting from ginning (CR), both sourced from private enterprises in Central Greece. The raw materials were air-dried, processed through riffling, ground using a cutting mill, and then sieved to achieve a particle size of less than 200 μm.

Fuel characterization was performed following the European standards set by CEN/TC335. Programmable laboratory furnaces were used for proximate analysis, while a CHNS analyzer model Thermo Scientific Flash 2000 was used for ultimate analysis. The calorific value was determined using a Leco AC-300 bomb calorimeter. The specific surface area was assessed using liquid nitrogen adsorption data at relative pressures ranging from 0.03 to 0.3, following the BET methodology.

Samples were out-gassed at 150°C under vacuum overnight and analyzed with an automatic Nova 2200 from Quantachrome. The inorganic chemical elements present in the fuel ashes were analyzed using an X-ray fluorescence spectrometer, specifically the S2 Ranger/EDS model from Bruker AXS.

2.2 Experiments under a Carbon Dioxide Atmosphere

The experimental setup consisted of a thermogravimetric analyzer TG/DTG from Perkin Elmer, coupled with a mass spectrometer, model QME-200 from Baltzers. The microbalance had a sensitivity of less than 5 μg, an accuracy of 0.2% wt, and a temperature precision of ±2°C. The heating rates varied from 5 to 50°C/min, while the flow rate of CO_2 was set at 35 mL/min. For the pyrolysis tests, samples weighing 10-15 mg were heated up to 600°C, and for the gasification tests of the chars, they were heated up to 950°C until a stable weight was achieved.

By processing the TG and DTG curves, key process parameters were extracted, including initial, peak, and final temperatures (T_i, T_{max}, and T_f, respectively), maximum weight loss rate (R_{max}), reactivity calculated as R_{max}/T_{max}, and conversion rates. The reproducibility of the experiments was validated by calculating the relative standard deviation (RSD) from repeated tests.

Gasification products were analyzed online using a mass spectrometer. The transfer line connecting the TG/DTG system and the MS was made of fused silica capillary tubing (i.d. 0.32 mm), insulated, and heated to 200°C to avoid condensation of the volatile compounds. The Secondary Electron Multiplier functioned at 82 eV, and the atomic mass detection range was 1-400. Data acquisition was managed by Pyris v3.5 and Quadstar 422 software, which accounted for all fragments corresponding to each m/z ratio. High-purity standard gases with known concentrations in argon were employed to establish calibration factors.

3. Kinetic Modeling

3.1 Independent Parallel Reactions Model (IPR Model)

The Independent Parallel Reactions model (IPR) was employed to analyze the kinetics of CO_2 pyrolysis and gasification. In pyrolysis, multiple pseudo-components were identified, representing various materials that decompose at different temperature ranges, including hemicellulose, cellulose, and lignin. The thermal degradation of these pseudo-components involved overlapping independent partial reactions. The decomposition of materials was described by the extent of conversion with time of n-th order differential equations, each with a unique couple of kinetic parameters (pre-exponential factor, activation energy). For gasification, due to the heterogeneous nature of the char, it was assumed that the char sample was a blend of several pseudo-components. The reactivity of each component can be expressed by the following kinetic equation [4, 29]:

$$\frac{da_i}{dt} = A_i \times e^{-\frac{E_i}{RT}} \times P_{CO_2} \times f(a_i) \quad (1)$$

In this equation, A_i and E_i denote the pre-exponential factor and activation energy for component i, respectively, while a_i signifies the conversion. P_{CO_2} refers to the partial pressure of CO_2 and v represents the reaction order concerning the gas partial pressure. The function $f(a_i)$ is defined as follows:

$$f(a_i) = (1 - a_i)^{n_i} \tag{2}$$

This function describes how the surface reactivity of the i-th component varies with its fractional conversion in a reaction of order n_i. The overall mass rate of the biochar sample is then determined by:

$$\frac{dm}{dt} = \sum_{i=1}^{k} c_i \times \frac{da_i}{dt} \quad i=1...k \tag{3}$$

where c_i indicates the contribution of component i to the total degradation. The process for calculating the kinetic parameters is elaborated in earlier research [18].

3.2 Distributed Activation Energy Model (DAEM Model)

In the Distributed Activation Energy Model (DAEM) model, biomass comprises one or more pseudo-components, similar to the IPR model. However, each component consists of fractions that share a common pre-exponential factor but have differing activation energies that follow a Gaussian distribution. The varying activation energy denotes the different reactivities of the fractions involved. Assuming the partial pressure of CO_2 is equal to 1 and that each fraction undergoes an n-order decomposition, the conversion for the m-th fraction of pseudo-component I can be calculated as follows [4, 29]:

$$a_m(T, E) = 1 - e^{-\frac{A}{b}\int_{T_o}^{T} e^{\frac{E_i}{RT}}dT} \tag{4}$$

The overall conversion of component i is determined by integrating the activation energy from 0 to ∞:

$$a_i(T) = 1 - \int_0^{\infty} e^{-\frac{A_i}{b}\int_{T_o}^{T} e^{\frac{E_i}{RT}}dT} \times f(E)dE \tag{5}$$

$$a_m(T, E) = 1 - e^{-\frac{A}{b}\int_{T_o}^{T} e^{\frac{E_i}{RT}}dT} \tag{6}$$

where f(E) is defined by the Gaussian distribution function:

$$f(E) = \frac{1}{\sigma \times \sqrt{\pi}} \times e^{\frac{-(E-E_o)^2}{2\sigma^2}} \tag{7}$$

In equation (6) E_o is the mean activation energy and σ is the standard deviation.

The approach for optimally fitting the experimental data is detailed in a previous study [18].

4. Results and Discussion

4.1 Fuel Analyses

A comparison of proximate and ultimate analyses, calorific value, and specific surface area for the raw fuels and the chars obtained after the pyrolysis process is made in Table 1. Raw samples had similar volatiles, fixed carbon and ash contents, resulting in a similar and significant calorific value and highly oxygenated. Sulfur concentration was very low. However, the nitrogen concentration was relatively high, especially the one corresponding to SP fuel, implying some nitrogenous emissions, such as NH_3, during the pyrolysis and gasification processes.

Table 1 Characterization of raw materials and chars (% dry).

Sample	Volatiles	Fixed Carbon	Ash	C	H	N	O	S	HHV (MJ/kg)	Specific Surface Area (m^2/g)
SP raw	73.5	19.6	6.9	43.0	6.3	2.7	40.9	0.2	18.0	1.9
char	-	80.0	20.0	45.4	1.5	1.4	31.7	-	16.5	28.0
CR raw	75.7	15.8	8.5	41.8	6.0	0.9	42.6	0.2	17.9	2.1
char	-	73.2	26.8	65.6	1.8	0.6	5.2	-	32.8	57.5

After thermal decomposition up to 600°C, Table 1 shows that hydrogen and oxygen volatile species evolved, leaving a char material enriched in carbon and minerals. The drop in the oxygen content of CR char was marked so that it effectively doubled its calorific value compared to the initial measurement. Furthermore, the specific surface area increased by 15 to 27 times following thermal treatment.

From the analysis of fuel ashes in Figure 1, it can be observed that both ashes were rich in Ca, Mg, and P. However, the ash of the CR had a remarkable content of K, too, probably related, together with P content, to fertilizer application during the cultivation of these plants. Alkali metals, particularly K and Na, are known to enhance catalytic activity during the gasification process [6, 30, 31].

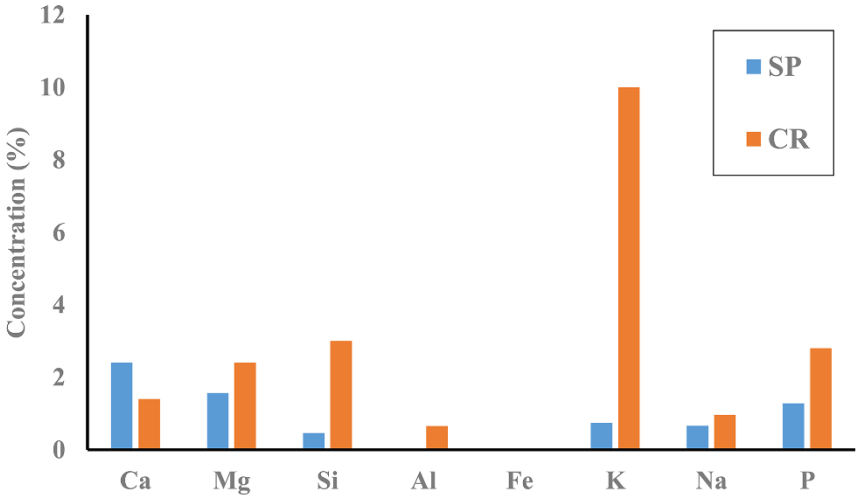

Figure 1 Chemical analysis of fuel ashes.

4.2 Pyrolysis Process

4.2.1 Thermal Decomposition Characteristics

The pyrolysis deconvolution profiles of the raw samples under an atmosphere of carbon dioxide up to 600°C and the characteristic parameters are represented in Figure 2 and Table 2, respectively. Thermal decomposition of SP started earlier than that of CR fuel, at about 200°C, and the peak was obtained at a lower temperature with a higher reaction rate. The significant weight loss occurred between 250°C and 400°C, displayed by a single peak, reflecting the decomposition of cellulose and hemicellulose components. The tailing curve up to 600°C demonstrates the decomposition of lignin. The reactivity of the pyrolysis process, as defined by the R_{max}/T_{max} ratio, was somehow higher for the SP sample due to its greater content in cellulose, as will be shown below.

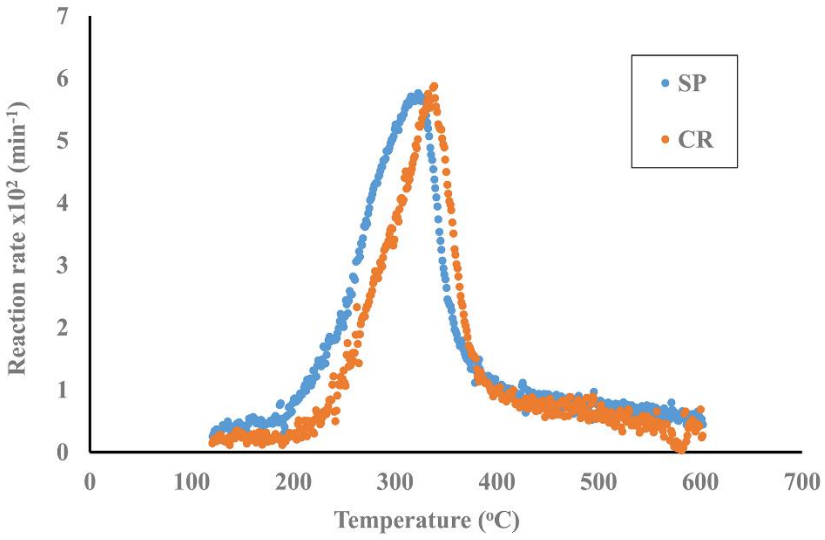

Figure 2 Pyrolysis deconvolution profiles of raw samples.

Table 2 Characteristic parameters of pyrolysis.

Sample	T_i (°C)	T_{max} (°C)	$R_{max} \times 10^2$ (min^{-1})	$R_{max}/T_{max} \times 10^4$ (min^{-1} C^{-1})
SP	197	322	5.85	1.81
CR	225	338	5.72	1.69

4.2.2 Kinetic Analysis

Using the IPR model, three first-order reactions were identified as effectively characterizing the process (Figure 3, Table 3). The first reaction, occurring between 250°C and 370°C, was attributed to the degradation of hemicelluloses. The second reaction, spanning 200°C to 420°C, corresponded to the breakdown of cellulose, while the third reaction, which took place over a broad temperature range of 150°C to 600°C, was associated with lignin degradation. The principal cellulose component accounted for 38% of the pyrolysis of the SP sample and 31% of the CR sample. These model values were derived according to the thermal decomposition domain, the shape, and the width of the pyrolysis pseudo-components. Results obtained by the TGA method, which has a high potential for

rapid and accurate analysis, agree with typical hydrolysis methods [21]. Cellulose content reported for other agricultural materials was between 31% and 52% [21, 32]. The deviation values between the computed and experimental data, obtained through a gradient-based minimization function in Matlab code, ranged from 1.6% to 2.4% at a heating rate of 10°C/min, increasing to up to 3.7% at higher heating rates, indicating the effectiveness, the reliability, and flexibility of the model. Activation energy values in Table 3, ranging from 17 kJ/mol to 165 kJ/mol, were comparable for both fuels and aligned with previously reported values in the literature for lignocellulosic materials [14, 15, 18, 21-23]. The lower activation energy corresponding to the lignin pseudo-component reveals its early degradation at low temperatures. The model was also validated by the authors through application to other biomass materials, such as olive by-products, vine shoots, sewage sludge, and animal sludge, as well as under different experimental conditions, such as heating rates [18].

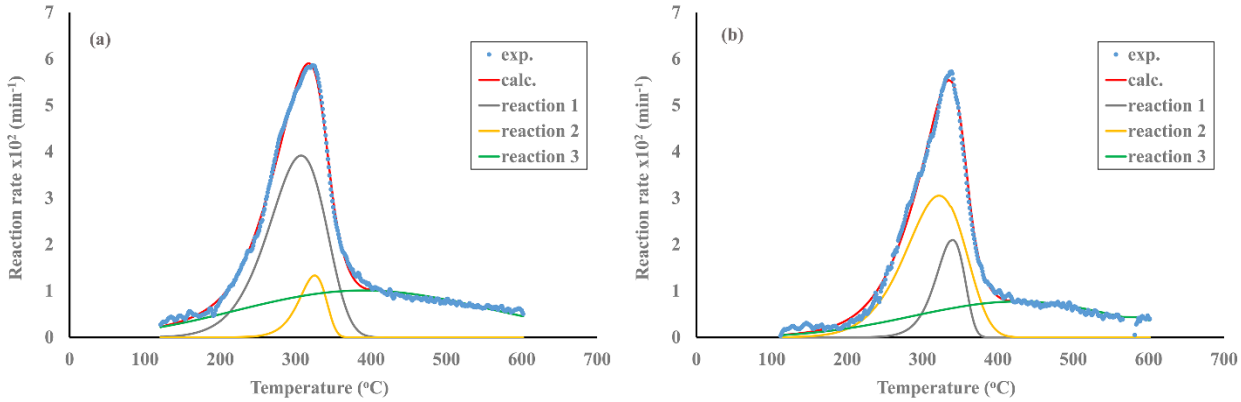

Figure 3 Kinetic analysis with IPR model of (a) SP and (b) CR fuels for the pyrolysis process.

Table 3 Kinetic parameters of pyrolysis.

IPR model							
Sample	**Reaction**	**A (min^{-1})**	**E (kJ/mol)**	**c (%)**	**n**	**σ (kJ/mol)**	**dev (%)**
SP	1	4.4×10^5	69	38	1		
	2	1.3×10^{14}	165	6.3	1		1.6
	3	1.1	17	39	1		
CR	1	4.0×10^5	71	31	1		
	2	6.0×10^{13}	165	10	1		2.4
	3	4.7	25	25	1		
DAEM model							
SP	1	1.7×10^{13}	177	39	1	4.38	
	2	3.7×10^{13}	151	26	1	0.95	1.6
	3	3.1×10^{14}	170	13	1	0.25	
CR	1	2.3×10^{15}	146	31	1	0.27	
	2	4.5×10^{14}	165	10	1	3.23	2.1
	3	3.2×10^{15}	170	25	1	0.48	

Similarly, the DAEM model also required three first-order reactions to describe the decomposition of the fuels during pyrolysis effectively. As shown in Figure 4 and Table 3, the contribution of the second reaction for the SP sample, related to the hemicellulose component, was more significant than the one determined by the IPR model (26% vs. 6.3%). The optimal parameters A, E, σ, and c for this model were determined using Matlab code as before, with numerical calculations for the integral in equation (5). Kinetic value triplets (A, E, σ) were calculated for each pseudo-component. Numerous trials with varying initial values were conducted to achieve optimal parameters. The deviation values for the DAEM model were nearly identical to those calculated for the IPR model. The primary distinction between the two models is that the DAEM model predicted much higher pre-exponential factors and activation energy values (151-177 kJ/mol compared to 17-165 kJ/mol). This discrepancy is attributed to the mathematical compensation effect inherent in the DAEM model, i.e., the same changing trend of pre-exponential factor and activation energy, as well as the inclusion of the additional parameter σ, which describes the broad, low shape pattern of lignin pseudo-component without adjusting the activation energy value. Although current kinetic parameters are in accordance with literature data [15, 18, 24, 25, 33], the DAEM model has notable drawbacks compared to the IPR model, including a greater number of parameters to be tuned and, therefore, reduced computational efficiency, increased degrees of freedom during data fitting contributing to ill-conditioning and less realistic activation energy values for low-temperature pyrolysis processes. As a result, the IPR model is recommended for use over the more complex DAEM model in kinetic evaluations of biomass pyrolysis processes. DAEM model could be more accurate for non-woody species [18].

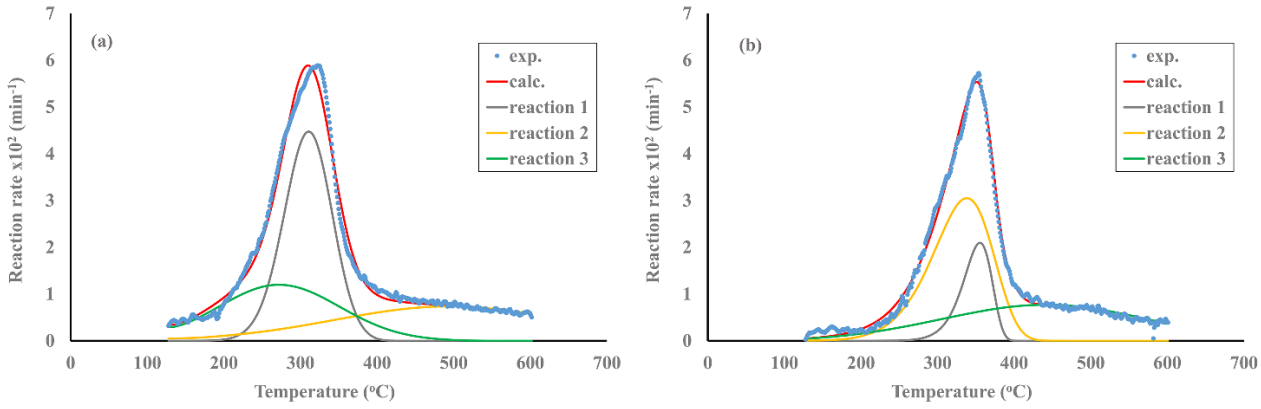

Figure 4 Kinetic analysis with DAEM model of (a) SP and (b) CR fuels for the pyrolysis process.

4.3 Gasification Process

4.3.1 Thermal Decomposition Characteristics

Figure 5 displays the DTG gasification profiles for the two chars in a carbon dioxide environment heated to 1000°C, whereas Table 4 provides a summary of the characteristic parameters obtained after processing of the thermograms, along with the composition of the product gas monitored by the MS system, the higher heating value of the gas and the conversion factor. As can be noticed from Figure 5, the Boudouard reaction commenced at temperatures exceeding 650°C, with the gasification process occurring at high temperatures peaking at around 900°C for both fuels. Notably,

the maximum rate of the CR sample was significantly higher than that of the SP sample, indicating that reactivity followed the trend of CR > SP. Organic matter conversion was complete in all instances. The increased reactivity of the CR char is correlated to its greater specific surface area developed during the pyrolysis process (Table 1), as well as its elevated amount in potassium (Figure 1), which appears that it exhibited a catalytic effect during the carbon dioxide gasification process. Additionally, Table 4 indicates that the higher heating value of the gas produced was nearly identical for both fuels, as the primary component of the gas was CO, along with traces of H_2, H_2O, CH_4, and various C_xH_y.

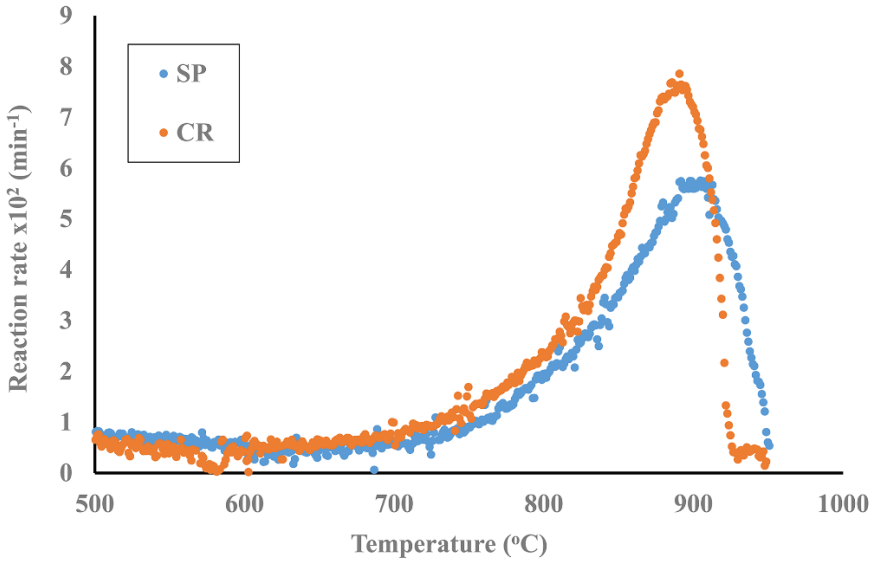

Figure 5 DTG gasification profiles of chars.

Table 4 Characteristic parameters of gasification.

Sample		**SP**	**CR**
T_i (°C)		675	657
T_{max} (°C)		905	891
$R_{max} \times 10^2$ (min^{-1})		5.65	7.85
$R_{max}/T_{max} \times 10^4$ (min^{-1} C^{-1})		0.62	0.88
	CO	97.7	93.2
	H_2O	-	5.0
Gas (% mol)	H_2	2.0	1.5
	CH_4	0.1	0.1
	C_xH_y	0.2	0.2
HHV (MJ/m^3)		12.8	12.2
Conversion (% daf)		100	100

4.3.2 Kinetic Analysis

The simulated DTG curves by the IPR model are compared with the experimental curves in Figure 6, and the kinetic parameters are included in Table 5. Gasification of SP and CR chars was successfully modeled by one pseudo-component. The fit was notably better for the SP fuel, with a deviation value of 2.3%, as opposed to the CR fuel, for which this value was 5%. The activation energy values presented in Table 5 are higher than those determined for the pyrolysis process, implying the enhanced aromaticity and thermal stability of the chars after devolatilization at high temperatures. Moreover, the increase of the pre-exponential factor with an increase in activation energy points to the compensation effect. The drop in the activation energy of the CR char, as compared to the SP char, confirms the higher reactivity of this fuel due to its larger specific surface area available for reaction and its greater content of inherent alkali elements, such as potassium, acting as catalysts for the process.

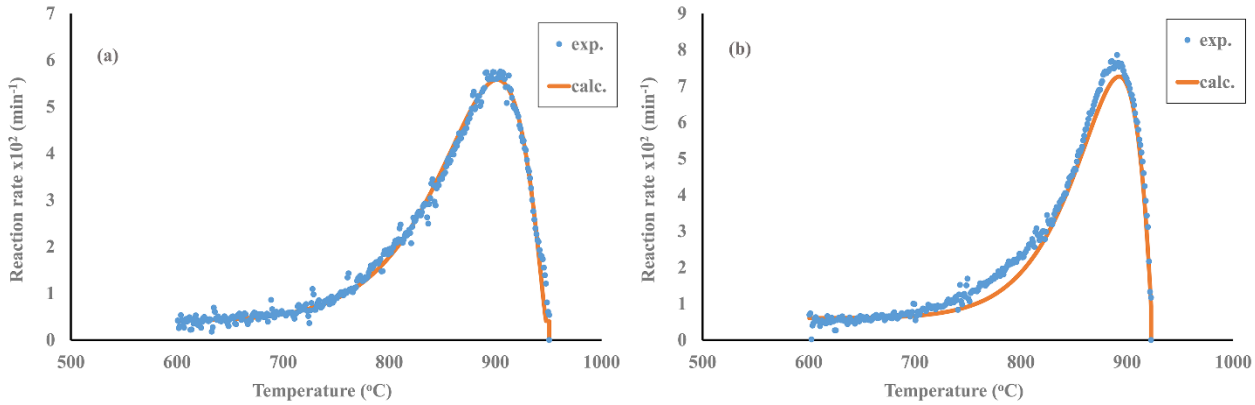

Figure 6 Kinetic analysis with IPR model of (a) SP and (b) CR chars for the gasification process.

Table 5 Kinetic parameters of gasification.

IPR model							
Sample	**Reaction**	**A (min^{-1})**	**E (kJ/mol)**	**c (%)**	**n**	**σ (kJ/mol)**	**dev (%)**
SP	1	1.5×10^{8}	201	100	0.55		2.3
CR	1	5.5×10^{5}	148	100	0.28		5.0
DAEM model							
SP	1	1.5×10^{9}	223	100	0.55	2.83	4.5
CR	1	3.3×10^{8}	207	100	0.28	2.21	5.0

In the case of the DAEM model, as illustrated in Figure 7, a single pseudo-component was also sufficient to describe the process. However, the fit of the simulated data to the experimental results was not as strong as with the IPR model, with deviation values between 4.5% and 5%. The compensation effect was also observed here, with estimated activation energy values being higher than those predicted by the IPR model. Therefore, the IPR model, providing better accuracy and fit and faster performance, is suggested for use in biomass gasification processes. Despite the variety of the materials used, the assumptions, and the mathematical establishment of these models, the kinetic parameters reported by previous investigations analyzing lignocellulosic materials and

agricultural wastes are in agreement with current values [9, 14, 19, 30, 33], confirm the reliability of the model and indicate that the process is chemically controlled.

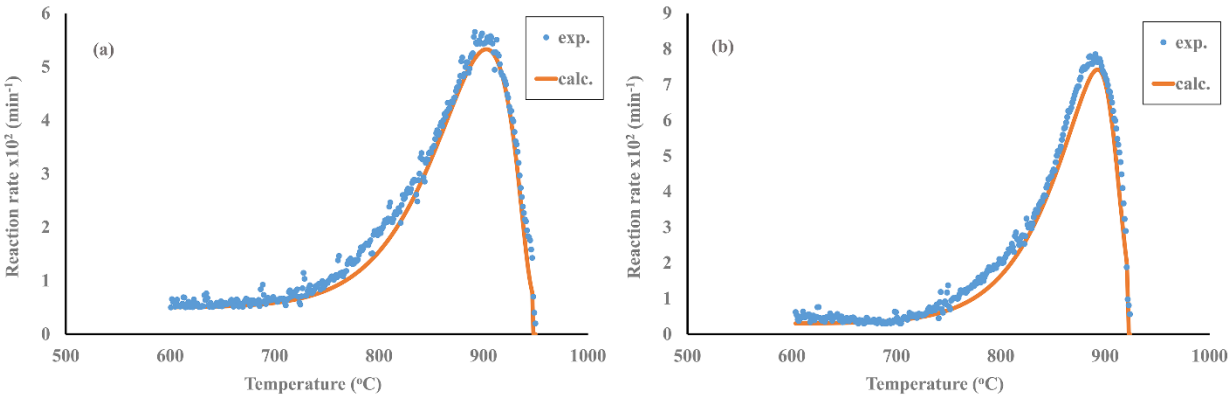

Figure 7 Kinetic analysis with DAEM model of (a) SP and (b) CR chars for the gasification process.

The kinetic models developed in the current study provide key data on the complex pyrolysis mechanism and gasification of some agricultural biomass materials using simple TGA experiments. The equations and algorithms described can also be applied to simulate the pyrolysis or gasification of other biomass materials and optimize the process operating conditions. However, they are restricted at very high heating rates. The kinetic results can be used for modeling these processes on a larger scale and are essential for the effective design of pyrolysis and gasification reactors for industrial applications.

5. Conclusions

The sunflower pomace and cotton residue fuels studied presented similar chemical compositions. During thermal decomposition with carbon dioxide agent, the reactivity of sunflower pomace fuel was higher due to its greater content in cellulose component.

Both the IPR and DAEM models accurately represented the pyrolysis process up to 600°C, with deviation values ranging from 1.6% to 2.4%. The activation energy values varied from 17 kJ/mol to 177 kJ/mol.

The gasification occurred between 650°C and 950°C, resulting in complete conversion of the chars. Cotton residue's reactivity was higher due to its larger specific surface area and higher levels of catalytic potassium.

The gasification process was effectively modeled using one pseudo-component, with deviation values between 2.3% and 5%, with the IPR model providing a superior fit. Activation energy values estimated from the DAEM model were higher than those from the IPR model (207-223 kJ/mol compared to 148-210 kJ/mol).

Overall, the developed IPR model, considering n-th order reaction mechanisms, was found to be more accurate, simpler and faster to implement. The kinetic results can be used for modeling these processes in a larger scale and are essential for the effective design of pyrolysis and gasification reactors for industrial applications.

Acknowledgement

The authors kindly thank the laboratories of Hydrocarbons Chemistry, Ore Beneficiation and Geochemistry, of the Technical University of Crete, for the ultimate analysis, BET and XRF analyses.

Author Contributions

D.V. Conceptualization, writing—review and editing, supervision, S.S. modeling, software, E.P. data curation, software.

Competing Interests

The authors have declared that no competing interests exist.

References

1. Choudhury T, Kayani UN, Gul A, Haider SA, Ahmad S. Carbon emissions. Environmental distortions and impact on growth. Energy Econ. 2023; 126: 107040.
2. Mulvaney D. Green new deal. Berkeley, CA: California Press; 2019.
3. Lahijani P, Zainal Z, Mohammadi M, Mohamed A. Conversion of the greenhouse gas CO_2 to the fuel gas CO via the Boudouard reaction: A review. Renew Sustain Energy Rev. 2015; 41: 615-632.
4. Chew J, Soh M, Sunarso J, Yong S, Doshi V, Bhattacharya S. Isothermal kinetic study of CO_2 gasification of torrefied oil palm biomass. Biomass Bioenergy. 2020; 134: 105487.
5. Lampropoulos A, Kaklidis N, Athanasiou C, Montes-Moran MA, Arenillas A, Menendez JA, et al. Effect of olive kernel treatment (torrefaction vs. slow pyrolysis) on the physicochemical characteritics and the CO_2 or H_2O gasification performance of as-prepared biochars. Int J Hydrog Energy. 2021; 46: 29126-29141.
6. Vamvuka D, Teftiki A, Sfakiotakis S. Increasing the reactivity of waste biochars during their co-gasification with carbon dioxide using catalysts and bio-oils. Thermochim Acta. 2021; 704: 179015.
7. Maya JC, Macias R, Gomez CA, Chejne F. On the evolution of pore microstructure during coal char activation with steam/CO_2 mixtures. Carbon. 2020; 158: 121-130.
8. Wang M, Wan Y, Guo Q, Bai Y, Yu G, Liu Y, et al. Brief review on petroleum coke and biomass/coal co-gasification: Syngas production, reactivity characteristics and synergy behavior. Fuel. 2021; 304: 121517.
9. Tian H, Wei Y, Cheng S, Huang Z, Qing M, Chen Y, et al. Optimizing the gasification reactivity of biochar: The composition, structure and kinetics of biochar derived from biomass lignocellulosic components and their interactions during gasification process. Fuel. 2022; 324: 124709.
10. Vamvuka D, Sfakiotakis S, Mpoumpouris A. Slagging and fouling propensities of ashes from urban and industrial wastes. Recent Innov Chem Eng. 2018; 11: 145-158.
11. Wei J, Wang M, Xu D, Shi L, Li B, Bai Y, et al. Migration and transformation of alkali/alkaline earth metal species during biomass and coal co-gasification: A review. Fuel Process Technol. 2022; 235: 107376.

12. Jayaraman K, Gokalp I, Petrus S, Belandria V, Bostyn S. Energy recovery analysis from sugar cane bagasse pyrolysis and gasification using thermogravimetry, mass spectrometry and kinetic models. J Anal Appl Pyrolysis. 2018; 132: 225-236.
13. He Q, Ding L, Raheem A, Guo Q, Gong Y, Yu G. Kinetics comparison and insight into structure-performance correlation for leached biochar gasification. Chem Eng J. 2021; 417: 129331.
14. Kartal F, Ozveren U. Novel multistage kinetic models for biomass pyrolysis and CO_2 gasification by means of reaction pathways. Bioresour Technol Rep. 2021; 15: 100804.
15. Kumar P, Subbarao PM, Kala LD, Vijay VK. Thermogravimetry and associated characteristics of pearl millet cob and eucalyptus biomass using differential thermal gravimetric analysis for thermochemical gasification. Therm Sci Eng Prog. 2021; 26: 101104.
16. Dong L, Alexiadis A. Simulation of char burnout characteristics of biomass/coal blend with a simplified single particle reaction model. Energy. 2023; 264: 126075.
17. Sun Y, Cai D, Yang Y, Chen X, Wang B, Yao Z, et al. Investigation of the thermal conversion behavior and reaction kinetics of the pyrolysis of bio-based polyurethane: A reference study. Biomass Bioenergy. 2023; 169: 106681.
18. Sfakiotakis S, Vamvuka D. Development of a modified independent parallel reactions kinetic model and comparison with the distributed activation energy model for the pyrolysis of a wide variety of biomass fuels. Bioresour Technol Rep. 2015; 197: 434-442.
19. Diedhiou A, Ndiaye L, Bensakhria A, Sock O. Thermochemical conversion of cashew nut shells, palm nut shells and peanut shells char with CO_2 and/or steam to aliment a clay brick firing unit. Renew Energy. 2019; 142: 581-590.
20. Brillard A, Brilhac JF. Improvements of global models for the determination of the kinetic parameters associated to the thermal degradation of lignocellulosic materials under low heating rates. Renew Energy. 2020; 146: 1498-1509.
21. Sophonrat N, Wooldridge M. Revisiting biomass compositions determination using thermogravimetric analysis and independent parallel reaction model. Thermochim Acta. 2024; 739: 179814.
22. Lopes FC, Tannous K, Carmazini EB. Thermal behavior and kinetic analysis of torrefied coconut fiber pyrolysis. Thermochim Acta. 2022; 715: 179275.
23. Siddiqi H, Kumari U, Biswas S, Mishra A, Meikap BC. A synergistic study of reaction kinetics and heat transfer with multi-component modeling approach for the pyrolysis of biomass waste. Energy. 2020; 204: 117933.
24. Mishra RK, Naik SU, Chistie SM, Kumar V, Narula A. Pyrolysis of agricultural waste in a thermogravimetric analyzer: Studies of physicochemical properties, kinetics behavior and gas compositions. Mater Sci Energy Technol. 2022; 5: 399-410.
25. Fatmawati A, Nurtono T, Widjaja A. Thermogravimetric kinetic-based computation of raw and pretreated coconut husk powder lignocellulosic composition. Bioresour Technol Rep. 2023; 22: 101500.
26. Wang J, Mingshen J, Zhang P, Liu Q, Zhang S, Wang K, et al. Elucidating kinetic mechanisms of lignin and biomass pyrolysis by distributed activation energy model with genetic algorithm. Energy. 2024; 312: 133548.
27. Yang Y, Jiang M, Song L, Shen Y, Lei T, Cai J. Systematical analysis and application of distributed activation energy model (DAEM) with Weibull distribution for pyrolysis kinetics of lignocellulosic biomass. Renew Energy. 2024; 237: 121549.

28. Fu Z, Xue Y, Li J, Yan B, Han Z, Chen G. Steam gasification of yak manure: Kinetic modeling by a sequential and coupling method. Fuel. 2022; 329: 125464.
29. Tannous K, Oliveira T. Tucumã endocarp pyrolysis kinetics: A comparative analysis between independent parallel and consecutive reactions schemes. Bioresour Technol Rep. 2022; 18: 101078.
30. Gupta A, Thengane S, Mahajani S. CO_2 gasification of char from lignocellulosic garden waste: Experimental and kinetic study. Bioresour Technol. 2018; 263: 180-191.
31. Ramos A, Monteiro E, Silva V, Rouboa A. Co-gasification and recent developments on waste-to-energy conversion: A review. Renew Sustain Energy Rev. 2018; 81: 380-396.
32. Kim H, Yu S, Kim M, Ryu C. Progressive deconvolution of biomass thermogram to derive lignocellulosic composition and pyrolysis kinetics for parallel reaction model. Energy. 2022; 254: 124446.
33. Yousef S, Eimontas J, Striugas N, Abdelnaby MA. Pyrolysis and gasification kinetic behavior of mango seed shells using TG-FTIR-GC-MS system under N_2 and CO_2 atmospheres. Renew Energy. 2021; 171: 733-749.